Synergistic cues from diverse bacteria enhance multicellular development in a choanoflagellate

Running title:

5   **Synergistic bacterial cues enhance multicellularity**

Ella V. Ireland[a], Arielle Woznica[a,*] and Nicole King[a,b#]

[a]Department of Molecular and Cell Biology, University of California, Berkeley,

10   California, USA

[b]Howard Hughes Medical Institute, University of California, Berkeley, California, USA

#Address correspondence to Nicole King, nking@berkeley.edu.

*Present address: Department of Microbiology, University of Texas Southwestern

15   Medical Center, Dallas, Texas, USA

Abstract

Bacteria regulate the life histories of diverse eukaryotes, but relatively little is known about how eukaryotes interpret and respond to multiple bacterial cues encountered simultaneously. To explore how a eukaryote might respond to a combination of bioactive molecules from multiple bacteria, we treated the choanoflagellate *Salpingoeca rosetta* with two sets of bacterial cues, one that induces mating and the other that induces multicellular development. We found that simultaneous exposure to both sets of cues enhanced multicellular development in *S. rosetta*, eliciting both larger multicellular colonies and an increase in the number of colonies. Thus, rather than conveying conflicting sets of information, these distinct bacterial cues synergize to augment multicellular development. This study demonstrates how a eukaryote can integrate and modulate its response to cues from diverse bacteria, underscoring the potential impact of complex microbial communities on eukaryotic life histories.

Importance

Eukaryotic biology is profoundly influenced by interactions with diverse environmental and host-associated bacteria. However, it is not well understood how eukaryotes interpret multiple bacterial cues encountered simultaneously. This question has been challenging to address because of the complexity of many eukaryotic model systems and their associated bacterial communities. Here, we studied a close relative of animals, the choanoflagellate *Salpingoeca rosetta*, to explore how eukaryotes respond to diverse bacterial cues. We found that a bacterial

2

chondroitinase that induces mating on its own can also synergize with bacterial lipids that induce multicellular "rosette" development. When encountered together, these cues enhance rosette development, resulting in the formation of more rosettes, each containing more cells than rosettes that form in the absence of the

45   chondroitinase. These findings highlight how synergistic interactions among bacterial cues can influence the biology of eukaryotes.

Introduction

Eukaryotes, including animals and their closest living relatives, choanoflagellates, encounter abundant and diverse bacteria in the environment (1–

50   3). However, interactions among eukaryotes and bacteria can be challenging to study in animal models due to the complex physiology of the hosts and the large number of oftentimes unculturable bacteria present, each of which releases diverse molecules (4–6). Multiple types of intestinal bacteria are required to induce full immune maturation in mice and humans, but it remains unclear whether this is due

55   to interactions among the bacteria, or the integration by the host of multiple independent bacterial cues (7–11). The interaction of a eukaryote with multiple partners can change the magnitude or directionality of each pair-wise interaction (12), and it can be challenging to measure the functional and fitness effects of such complex networks (13). Therefore, simpler model systems may be necessary to

60   investigate how animals and other eukaryotes integrate information from multiple bacterial cues encountered at the same time.

The choanoflagellate *Salpingoeca rosetta* can serve as a simple model for studying interactions between bacteria and eukaryotes. Like all choanoflagellates, *S. rosetta* captures bacterial prey from the water column using an apical "collar

65   complex" composed of a microvillar collar surrounding a single flagellum (Fig. 1A; (14, 15)). In addition, like many animals (2, 16, 17), *S. rosetta* undergoes important life history transitions in response to distinct bacterial cues. For example, a secreted bacterial chondroitinase called EroS (for Extracellular Regulator of Sex) produced by *Vibrio fischeri*, *Proteus vulgaris,* and select other Gammaproteobacteria induces

4

70   solitary *S. rosetta* cells to gather into mating swarms (Fig. 1B; (18)). The cells in

mating swarms are not stably adherent and eventually resolve into pairs of cells

that mate by undergoing cell and nuclear fusion, followed by meiotic recombination.

When exposed to a different type of bacterial cue, specific sulfonolipids called RIFs

(for Rosette Inducing Factors) from the Bacteroidetes bacterium *Algoriphagus*

75   *machipongonensis,* solitary cells of *S. rosetta* undergo serial rounds of cell division

without separation, thereby resulting in the development of multicellular rosettes of

cells (Fig. 1C) that are physically linked by cytoplasmic bridges and a shared

extracellular matrix (19–22).

     Mating and rosette development in *S. rosetta* differ in many respects, including

80   the chemical nature of the bacterial cues (a protein versus lipids) and the underlying

cell biology (cell aggregation versus incomplete cytokinesis). Moreover, the time

scales of these processes differ, with mating swarms forming within 0.5 hours of

EroS treatment (18), while definitive rosettes require multiple rounds of cell

division and are not observed until 11 - 24 hours after exposure to RIFs (19–22).

85   Motivated by the existence of distinct *S. rosetta* life history transitions that can

be regulated by biochemically unrelated bacterial cues, we used *S. rosetta* as a

simple model for exploring how eukaryotes are influenced by environments filled

with diverse bacterial cues. We investigated how *S. rosetta* responds to

environments containing both the mating inducer EroS and the rosette-inducing

90   RIFs. We found that the initiation of mating behavior is unchanged in the presence

of cues that induce rosette development. In contrast, rosette development is

significantly enhanced by the presence of the mating inducer, revealing that *S.*

rosetta integrates information from seemingly unrelated bacterial cues during rosette development.

95

Results

Rosettes swarm in response to the EroS$_{Pv}$ mating factor

In a culture containing *S. rosetta* and the prey bacterium *Echinicola pacifica* (together comprising a culture called SrEpac; (23, 24)), solitary cells proliferated rapidly, but underwent no other observable cell state transitions (Fig. 1A). When the SrEpac culture was treated with the secreted bacterial chondroitinase EroS from *P. vulgaris* (EroS$_{Pv}$)*, S. rosetta* cells formed mating swarms of 2-50 cells within 0.5 hours (Fig. 1B, Table 1), as previously reported (18)*.* In contrast, treatment of SrEpac with *A. machipongonensis* RIFs contained in outer membrane vesicles (RIF-OMVs) induced development of multicellular rosettes within 24 hours (Fig. 1C, D, Table 1; (19, 22)).

We then tested how mature rosettes (formed in response to pre-treatment with RIF-OMVs for 24 hours) would respond to the mating inducer EroS. After treatment with EroS$_{Pv}$ for 0.5 hours, the pre-formed rosettes gathered into swarms that were quantifiable by their increase in area (median = 58.7 μm^2, interquartile range = 21.6-98.0 μm^2) as compared to untreated rosettes (median = 35.5 μm^2, interquartile range = 17.8-65.9 μm^2) (Fig. 1D-F, Table 1). Therefore, rather than being mutually exclusive, the rosette morphology induced by RIF-OMVs and the swarming behavior induced by EroS$_{Pv}$ are compatible. This indicates that cells in a life history stage induced by one bacterial cue (in this case RIF-OMVs) can respond to a second

6

bacterial cue (EroS$_{Pv}$). Swarms of choanoflagellate rosettes have not previously been reported, to our knowledge, and their ecological relevance is unknown.

<u>The mating inducer EroS$_{Pv}$ enhances rosette development</u>

120   We next investigated how single-celled *S. rosetta* in an SrEpac culture would respond to simultaneous exposure to EroS$_{Pv}$ and RIF-OMVs. SrEpac cultures treated solely with RIF-OMVs for 0.5 hours, considerably less time than that required for rosette development, did not produce swarms and were indistinguishable from untreated SrEpac cultures (Fig. S1A-C', Table 1; (18, 19)). Moreover, when SrEpac

125   cultures were treated simultaneously with EroS$_{Pv}$ and RIF-OMVs for 0.5 hours, the cells swarmed and the culture was indistinguishable from one treated with EroS$_{Pv}$ alone (Fig. S1A, D-E', Table 1). Therefore, RIF-OMVs do not appear to influence the swarm-inducing activity of EroS$_{Pv}$ over time scales of 0.5 hours or less.

In contrast, when SrEpac cultures were co-treated with RIF-OMVs and EroS$_{Pv}$ for

130   24 hours (long enough for rosettes to develop), the percentage of cells in rosettes increased markedly compared to cultures treated with RIF-OMVs alone (Fig. 2A, Table 1). Thus, EroS$_{Pv}$ enhances the rosette-inducing activity of RIF-OMVs. The enhancing activity of EroS$_{Pv}$ derived, in part, from the increased sensitivity of the culture to RIF-OMVs, allowing for rosette development at RIF-OMV concentrations

135   that would otherwise fail to elicit rosette development. For example, at a nearly 10^{-6} dilution of RIF-OMVs, no rosettes were detected in the RIF-OMV alone condition, while 4.5±0.8% (mean ± S.D.) of the cells in cultures co-treated with EroS$_{Pv}$ and RIF-OMVs were found in rosettes (see circle #1, Fig. 2A). In addition, when cells were

exposed to saturating concentrations of RIF-OMVs (dilutions ≥$3.7×10^{-4}$), co-

140   treatment with EroS$_{Pv}$ increased the percentage of cells in rosettes from a maximum

of 83.6±6.8% (mean ± S.D.) in cultures that were treated with RIF-OMVs alone to

92.6±0.3% (mean ± S.D.) in cultures co-treated with RIF-OMVs and EroS$_{Pv}$ (see circle

#2, Fig. 2A).

Enhancement of rosette development by the mating factor EroS was unexpected,

145   and we next sought to understand the phenomenon in greater detail. To that end,

we optimized a method for reproducibly inducing rosette development at low levels.

Treating SrEpac with a 1:20,000 dilution of RIF-OMVs drove only a small percentage

of cells (1-20%) into rosettes (Fig. 2A, Fig. S2A) and thereafter formed the basis of a

"sensitized rosette induction assay" in which we could quantify the influence of

150   EroS$_{Pv}$. Under the conditions of the sensitized rosette induction assay, we found that

EroS$_{Pv}$ enhanced rosette development in a concentration-dependent manner that

saturated at 0.05 U/mL (Fig. S2B). Using this sensitized rosette induction assay

across a time series, the rosette enhancing activity of EroS$_{Pv}$ at the population level

became more evident (Fig. S2C). For example, while treatment of SrEpac with

155   1:20,000 RIF-OMVs yielded only 23.4±4.9% (mean ± S.D.) of cells in rosettes at 39-

hours post-treatment, co-treatment with 1:20,000 RIF-OMVs and 0.05 U/mL EroS$_{Pv}$

yielded 88.2±2.7% (mean ± S.D.) of cells in rosettes (Fig. 2B).

These data demonstrated that co-treatment with EroS$_{Pv}$ increases the percentage

of cells in rosettes at a population level but did not reveal whether EroS$_{Pv}$-mediated

160   enhancement works by (1) increasing the overall number of rosettes, (2) increasing

the average number of cells per rosette, or (3) both. To test whether co-treatment

with EroS$_{Pv}$ increased the number of rosettes formed, we induced SrEpac with either

RIF-OMVs alone or RIF-OMVs + EroS$_{Pv}$ and measured the ratio of rosette colonies to

solitary cells. Co-treatment with RIF-OMVs and EroS$_{Pv}$ in the sensitized rosette

165 induction assay consistently increased the ratio of rosette colonies to solitary cells

throughout the time series. For example, at 39 hours post-treatment, the ratio of

rosettes to solitary cells after co-treatment with RIF-OMVs and EroS$_{Pv}$ was

0.96±0.31 (mean ± S.D.), compared to 0.06±0.02 (mean ± S.D.) after treatment with

RIF-OMVs alone (Fig. 2C). The ratio of rosettes to solitary cells eventually plateaued,

170 likely due to both solitary cells and rosettes (which can divide by fission (20))

dividing at the same rate. To test whether rosette size is influenced by co-treatment

with EroS$_{Pv}$, we used the sensitized rosette induction assay to compare the number

of cells per rosette in cultures treated with RIF-OMVs alone to those treated with

RIF-OMVs and EroS$_{Pv}$. Cultures co-treated with EroS$_{Pv}$ formed larger rosettes (with

175 8.9±2.7 (mean ± S.D.) cells per rosette colony at 39-hours post-treatment) compared

with those treated with RIF-OMVs alone (5.3±1.7 (mean ± S.D.) cells per rosette

colony at the same time point) (Fig. 2D). Importantly, co-treatment with EroS did

not affect the growth rate or cell density of cultures (Fig. S2D), indicating that the

increase in cell number per rosette was not due to a difference in cell division rates.

180 Therefore, at limiting concentrations of RIF-OMVs, EroS$_{Pv}$ enhances the rosette-

inducing activity of RIF-OMVs in at least two ways: at the population level, by

increasing sensitivity to RIFs and the number of cells that initiate rosette

development, and at the level of development, by increasing the maximal size of

rosettes.

9

185

<u>Purified RIFs and EroS are sufficient for enhancement of rosette induction</u>

Because *A. machipongonensis* OMVs contain a suite of proteins, sugars, the

sulfonolipid RIFs, and diverse other lipids, we next explored whether RIFs are

sufficient for EroS$_{Pv}$-mediated enhancement of rosette development or whether the

190   phenomenon requires a non-RIF. For example, certain

lysophosphatidylethanolamines (LPEs), lipids found alongside RIFs in *A.*

machipongonensis OMVs, synergize with RIFs and enhance rosette induction, in part

by increasing the resistance of larger rosettes to shear forces (22).

To test whether EroS$_{Pv}$ acts synergistically with RIFs or requires other

195   components of RIF-OMVs, we compared rosette development in SrEpac cultures

treated with high-performance liquid chromatography (HPLC)-purified RIFs (19,

22) with that in cultures co-treated with HPLC-purified RIFs and EroS$_{Pv}$. Co-

treatment with EroS$_{Pv}$ and purified RIFs caused a significant increase in the

percentage of cells in rosettes compared to purified RIFs alone, indicating that the

200   enhancement does not require other components of *A. machipongonensis* OMVs (Fig.

3A). Moreover, enhancement of rosette development was not restricted to *P.*

vulgaris EroS. Co-treatment with purified *V. fischeri* EroS (EroS$_{Vf}$) also significantly

enhanced RIF-OMV-induced rosette development (Fig. 3B), revealing that the

enhancing activity likely stems from the chondroitinase activity conserved between

205   EroS$_{Vf}$ and EroS$_{Pv}$ rather than from a lineage-specific feature found only in EroS$_{Pv}$.

These findings show that simultaneous exposure to just two bacterial cues, RIFs and

EroS, is sufficient to induce enhanced development of rosettes in *S. rosetta*.

10

Discussion

210   We have shown here that the choanoflagellate *S. rosetta* can sense and respond to a mix of bacterial cues, each of which in isolation induces a seemingly disparate life history transition – mating or multicellularity. Together, these cues enhance multicellular development, increasing the number of cells in rosettes at a population level by increasing the proportion of rosettes to single cells and by increasing the

215   number of cells per rosette (Fig. 2 and 4).

The *S. rosetta* targets for EroS and the sulfonolipid RIFs are as-yet unknown (18, 19), making it challenging to infer the specific mechanisms by which EroS might enhance rosette development. One possibility is that EroS may modify chondroitin sulfate proteoglycans through its chondroitinase activity, thereby improving access

220   of RIF receptors to RIFs, potentially explaining the increased sensitivity of EroS-treated *S. rosetta* to RIF-OMVs (Fig. 2A). This type of mechanism would resemble the regulation of vascular endothelial growth factor receptor 2 (VEGFR2), whose activity is inhibited by *N*-glycosylation; enzymatic digestion of glycans on VEGFR2 enhances its response to the VEGF ligand (25).

225   In addition to increasing the sensitivity of *S. rosetta* to RIF-OMVs, EroS treatment also resulted in rosettes that contained more cells (Fig. 2D). A link between rosette size and extracellular matrix (ECM) modification was previously reported for another colony-forming choanoflagellate, *Salpingoeca helianthica*, in which treatment with a bovine chondroitinase resulted in a significantly increased number

230   of cells per rosette (26). Furthermore, chemical perturbations of the *S. rosetta* ECM

and computational modeling have shown that the material properties of the ECM, such as stiffness and volume, exert a physical constraint on rosette volume and morphology (27). Thus, EroS digestion of chondroitin sulfate in the *S. rosetta* ECM may relax these constraints and allow for increased proliferation of cells within

235   rosettes.

Might *S. rosetta* in nature actually encounter the disparate types of bacteria that induce multicellularity and mating? Rosette development can be induced by diverse genera of marine bacteria, ranging from *A. machipongonensis*, which was co-isolated with *S. rosetta,* to *Zobellia uliginosa*, a macroalgal commensal (19, 28, 29)*.* Likewise,

240   mating can be induced by diverse *Vibrio* species (18), which are widespread in marine environments (30, 31). Moreover, the bioactive molecules produced by *A. machipongonensis* and *V. fischeri* (sulfonolipid RIFs and EroS) are secreted and are potent at ecologically relevant concentrations (femtomolar to nanomolar) that are comparable to those of other soluble marine signaling molecules (2, 18, 19, 22).

245   Taken together, the diversity and abundance of rosette-inducing and mating-inducing bacteria, and the potency of the molecules they produce, argue that RIFs and EroS could be simultaneously encountered by *S. rosetta* in nature. The synergy between these cues allows *S. rosetta* to sense and respond to significantly lower concentrations of rosette-inducing factors than it could otherwise (Fig. 2A),

250   contributing to the plausibility that the enhanced rosette induction they elicit could be ecologically relevant.

Simple host-microbe interactions, in which a single bacterium elicits a clear phenotype from a eukaryotic host, have begun to reveal the molecular mechanisms

12

by which bacteria influence the biology of eukaryotes. For example, *V. fischeri*

255   colonizes and is sufficient to induce the development of the light organ in the bobtail

squid, but this process only happens through the integration of multiple cues

produced by *V. fischeri* – peptidoglycan and lipopolysaccharide (32). Likewise, we

have previously shown that two types of molecules – sulfonolipid RIFs and specific

LPEs – are necessary to recapitulate the rosette-inducing activity of live *A.*

260   *machipongonensis* (22). Thus, interactions that are seemingly simple at the

organismal level – one bacterium and one eukaryote – can require complex

interactions at the molecular level.

Given the underlying molecular complexity of interactions involving only one

bacterium and one eukaryote, interactions among larger numbers of species are,

265   perhaps unsurprisingly, complex and can yield a variety of outcomes, including

synergistic effects (12). For example, arbuscular mycorrhizal fungi and rhizobia

bacteria individually confer beneficial effects on plants, and the simultaneous

presence of both groups in a tripartite association enhances these effects, increasing

plant biomass to a greater extent than each partner could alone (33). Synergistic

270   effects have also been demonstrated in interactions among eukaryotes and multiple

bacterial species, such as in polymicrobial infections. Direct interactions among

pathogens in polymicrobial infections (through metabolite exchange, signaling

molecules, or direct contact) can synergistically increase the disease burden for the

host (such as by increasing antibiotic resistance or virulence factor expression)

275   (34). Eukaryotic integration of bacterial cues has also been observed in the

mammalian immune system, in which immune receptors such as Toll-like receptors,

T cell receptors and co-receptors, each of which recognizes different bacterial ligands, synergize to enhance the response to multiple bacterial cues (35, 36).

280   Our finding that isolated cues from diverse environmental bacteria can synergize to enhance rosette development in *S. rosetta* (Fig. 3) demonstrates that this type of integration can occur at the level of the eukaryote, without requiring direct interactions among environmental bacteria. In the future, identifying the *S. rosetta* target(s) of RIF and EroS activity will likely provide detailed insights into the molecular mechanisms underlying EroS-mediated enhancement of rosette

285   development. The experimental tractability of *S. rosetta* and its susceptibility to the influences of environmental bacteria render it an exciting system in which to investigate the mechanisms by which eukaryotes grapple with a noisy and information-rich bacterial world.

Materials and Methods

290

<u>Choanoflagellate culturing conditions</u>

Artificial seawater (ASW) was prepared by diluting 32.9 g Tropic Marin sea salts in

1L water for a salinity of 32-37 parts per thousand (24). Sea Water Complete media

(SWC) was prepared by diluting 5 g/L peptone, 3 g/L yeast extract, and 3 mL/L

295   glycerol in ASW (24). SrEpac (*Salpingoeca rosetta* co-cultured with the prey

bacterium *Echinicola pacifica*, ATCC PRA-390; (24)) was cultured in 5% Sea Water

Complete media (5% SWC vol/vol in ASW) at 22ºC. Cultures were passaged daily, 1

mL into 9 mL fresh media in 25cm^2 cell culture flasks (Corning). Prior to rosette or

swarm induction, cultures were diluted to 1×10^5 choanoflagellate cells/mL in 5%

300   SWC and 100 μL volumes were aliquoted into a 96-well plate (Corning).

<u>Preparation of *A. machipongonensis* conditioned media and isolation of RIF-OMVs</u>

Outer membrane vesicles were isolated from *A. machipongonensis* as described in

(22). Briefly, *A. machipongonensis* (ATCC BAA-2233, (28)) was grown in 500 mL

305   100% SWC, shaking at 30ºC for 48 hours. The bacteria were pelleted and the

supernatant was filtered through a 0.2 μm filter to produce conditioned media.

Conditioned media was then centrifuged at 36,000 × g for 3 hours at 4ºC (Type 45 Ti

rotor, Beckman Coulter). OMV-containing pellets were resuspended in 2 mL ASW.

310   <u>HPLC purification of RIFs</u>

15

RIFs were purified by HPLC as described in (22). Briefly, *A. machipongonensis* was grown in 20 L Marine Broth media (Carl Roth (CP.73): 40.1 g/L), shaking at 30ºC for 48 hours. The cells were harvested by centrifugation and extracted with $CHCl_3$:MeOH (2:1, 4L). The organic extract was filtered and concentrated to give

315   approximately 3g crude lipid extract. The crude extract was dissolved in 60% MeOH ($+0.1\%$ NH_4OH) and fractionated using a C18-SPE (Solid Phase Extraction) using a 10% step-gradient of MeOH (60%-100% MeOH+0.1 NH_4OH). The resulting SPE fractions were analyzed for sulfonolipid-specific signals using LC-MS and ^{1}H-NMR. The fraction containing RIF-mix (RIF-1 and RIF-2) eluted with 90% MeOH (+0.1%

320   NH_4OH) during the SPE purification.

Rosette induction

Unless otherwise noted, SrEpac cultures were treated with a 1:1,000 dilution of RIF-OMVs and incubated for 24 hours before imaging or counting. To induce a low level

325   of rosette development in the sensitized rosette induction assay (Fig. 2B-D, Fig. 3B, Fig. S2B-D), SrEpac cultures were treated with a 1:20,000 dilution of RIF-OMVs. HPLC-purified RIFs were resuspended in DMSO and added at 10 µg/mL (Fig. 3A).

Swarm induction

330   Unless otherwise noted, cultures were treated with 0.05 U/mL chondroitinase ABC from *P. vulgaris* (Sigma), referred to as "EroS$_{Pv}$". EroS from *V. fischeri* (EroS$_{Vf}$; Fig. 3B) was purified as described in (18). Briefly, *V. fischeri* ES114 (ATCC 700601) was grown in 8 L 100% SWC, shaking at 20ºC for 30 hours. The bacteria were pelleted

and the supernatant was filtered through a 0.2 μm filter, concentrated to 120 mL

335   using a using a tangential flow filtration device with a 30 kDa Centramate filter (Pall

#OS030T12), then ammonium sulfate precipitated and further separated by size

exclusion chromatography. EroS$_{Vf}$ was added to SrEpac cultures at a final dilution of

0.1%.

340   Rosette quantification

To quantify the percentage of cells in rosettes, cultures were fixed with 1%

formaldehyde, vortexed, mounted on a Bright-Line hemacytometer (Hausser

Scientific), and counted on a Leica DMI6000B inverted compound microscope.

Rosettes were defined as groups of four or more cells, and were distinguished from

345   swarms based on their resistance to mechanical shear and their stereotypical

orientation with their basal poles pointed inwards and their flagella out (20, 23).

The numbers of solitary cells and rosettes, as well as the number of cells in each

rosette, were counted until at least 200 cells were scored (per biological replicate).

350   Swarm quantification

Cell cluster areas were quantified as described in (18). Briefly, samples were imaged

in 96-well glass-bottomed plates (Ibidi 89621) at 10× magnification using

transmitted light (bright field) on a Zeiss Axio Observer.Z1/7 Widefield microscope

with a Hammatsu Orca-Flash 4.0 LT CMOS Digital Camera. Images were processed

355   and analyzed in ImageJ as follows: 'Smooth' to reduce bacterial background, 'Find

Edges' to further highlight choanoflagellate cells, 'Make Binary' to convert to black

17

and white, 'Close-' to fill in small holes, and 'Analyze Particles' to calculate the area

of each cell cluster. Particles smaller than 10 μm^2 were removed to reduce

background bacterial signal.

360 **<u>Acknowledgements</u>**

References

1. McFall-Ngai MJ. 2002. Unseen forces: The influence of bacteria on animal development. Dev Biol 242:1–14.

370 2. Woznica A, King N. 2018. Lessons from simple marine models on the bacterial regulation of eukaryotic development. Curr Opin Microbiol 43:108–116.

3. McFall-Ngai M, Hadfield MG, Bosch TCG, Carey H V, Domazet-Lošo T, Douglas AE, Dubilier N, Eberl G, Fukami T, Gilbert SF, Hentschel U, King N, Kjelleberg S, Knoll AH, Kremer N, Mazmanian SK, Metcalf JL, Nealson K, Pierce NE, Rawls JF,

375 Reid A, Ruby EG, Rumpho M, Sanders JG, Tautz D, Wernegreen JJ. 2013. Animals in a bacterial world, a new imperative for the life sciences. Proc Natl Acad Sci 110:3229–3236.

4. Eckburg PB, Bik EM, Bernstein CN, Purdom E, Dethlefsen L, Sargent M, Gill SR, Nelson KE, Relman DA. 2005. Diversity of the human intestinal microbial

380 flora. Science 308:1635–1638.

5. Lozupone CA, Stombaugh JI, Gordon JI, Jansson JK, Knight R. 2012. Diversity, stability and resilience of the human gut microbiota. Nature 489:220–230.

6. Donia MS, Fischbach MA. 2015. Small molecules from the human microbiota. Science 349:1254766.

385 7. Tanoue T, Morita S, Plichta DR, Skelly AN, Suda W, Sugiura Y, Narushima S, Vlamakis H, Motoo I, Sugita K, Shiota A, Takeshita K, Yasuma-Mitobe K,

Riethmacher D, Kaisho T, Norman JM, Mucida D, Suematsu M, Yaguchi T, Bucci V, Inoue T, Kawakami Y, Olle B, Roberts B, Hattori M, Xavier RJ, Atarashi K, Honda K. 2019. A defined commensal consortium elicits CD8 T cells and anti-cancer immunity. Nature 565:600–605.

8.   Atarashi K, Tanoue T, Oshima K, Suda W, Nagano Y, Nishikawa H, Fukuda S, Saito T, Narushima S, Hase K, Kim S, Fritz J V, Wilmes P, Ueha S, Matsushima K, Ohno H, Olle B, Sakaguchi S, Taniguchi T, Morita H, Hattori M, Honda K. 2013. Treg induction by a rationally selected mixture of Clostridia strains from the human microbiota. Nature 500:232–236.

9.   Bouskra D, Brézillon C, Bérard M, Werts C, Varona R, Boneca IG, Eberl G. 2008. Lymphoid tissue genesis induced by commensals through NOD1 regulates intestinal homeostasis. Nature 456:507–510.

10. Martin R, Nauta AJ, Ben Amor K, Knippels LMJ, Knol J, Garssen J. 2010. Early life: Gut microbiota and immune development in infancy. Benef Microbes 1:367–382.

11. Chung H, Pamp SJ, Hill JA, Surana NK, Edelman SM, Troy EB, Reading NC, Villablanca EJ, Wang S, Mora JR, Umesaki Y, Mathis D, Benoist C, Relman DA, Kasper DL. 2012. Gut immune maturation depends on colonization with a host-specific microbiota. Cell 149:1578–1593.

12. Afkhami ME, Rudgers JA, Stachowicz JJ. 2014. Multiple mutualist effects: conflict and synergy in multispecies mutualisms. Ecology 95:833–844.

21

13.   Mushegian AA, Ebert D. 2016. Rethinking "mutualism" in diverse host-symbiont communities. BioEssays 38:100–108.

410   14.   Dayel MJ, King N. 2014. Prey Capture and Phagocytosis in the Choanoflagellate *Salpingoeca rosetta*. PLoS One 9:e95577.

15.   Leadbeater BSC. 2015. The collared flagellate: functional morphology and ultrastructure, p. 18–43. *In* The Choanoflagellates. Cambridge University Press, Cambridge.

415   16.   Tebben J, Tapiolas DM, Motti CA, Abrego D, Negri AP, Blackall LL, Steinberg PD, Harder T. 2011. Induction of Larval Metamorphosis of the Coral *Acropora millepora* by Tetrabromopyrrole Isolated from a *Pseudoalteromonas* Bacterium. PLoS One 6:e19082.

17.   Shikuma NJ, Pilhofer M, Weiss GL, Hadfield MG, Jensen GJ, Newman DK. 2014.
420   Marine Tubeworm Metamorphosis Induced by Arrays of Bacterial Phage Tail-Like Structures. Science 343:529–533.

18.   Woznica A, Gerdt JP, Hulett RE, Clardy J, King N. 2017. Mating in the closest living relatives of animals is induced by a bacterial chondroitinase. Cell 170:1–9.

425   19.   Alegado RA, Brown LW, Cao S, Dermenjian RK, Zuzow R, Fairclough SR, Clardy J, King N. 2012. A bacterial sulfonolipid triggers multicellular development in the closest living relatives of animals. eLife 1:e00013.

20.   Dayel MJ, Alegado RA, Fairclough SR, Levin TC, Nichols SA, McDonald K, King

430   N. 2011. Cell differentiation and morphogenesis in the colony-forming

          choanoflagellate *Salpingoeca rosetta*. Dev Biol 357:73–82.

21.   Fairclough SR, Dayel MJ, King N. 2010. Multicellular development in a

          choanoflagellate. Curr Biol 20:R875–R876.

22.   Woznica A, Cantley AM, Beemelmanns C, Freinkman E, Clardy J, King N. 2016.

          Bacterial lipids activate, synergize, and inhibit a developmental switch in

435   choanoflagellates. Proc Natl Acad Sci 113:7894–7899.

23.   Levin TC, Greaney AJ, Wetzel L, King N. 2014. The *rosetteless* gene controls

          development in the choanoflagellate *S. rosetta*. eLife 3:e04070.

24.   Levin TC, King N. 2013. Evidence for sex and recombination in the

          choanoflagellate *Salpingoeca rosetta*. Curr Biol 23:2176–2180.

440   25.   Chandler KB, Leon DR, Kuang J, Meyer RD, Rahimi N, Costello CE. 2019. N-

          glycosylation regulates ligand-dependent activation and signaling of vascular

          endothelial growth factor receptor 2 (VEGFR2). J Biol Chem

          jbc.RA119.008643.

26.   Richter DJ, Fozouni P, Eisen MB, King N. 2017. The ancestral animal genetic

445   toolkit revealed by diverse choanoflagellate transcriptomes. bioRxiv

          http://dx.doi.org/10.1101/211789.

27.   Larson BT, Ruiz-Herrero T, Lee S, Kumar S, King N. 2019. Biophysical

principles of choanoflagellate self-organization. bioRxiv

http://dx.doi.org/10.1101/659698.

450   28.   Alegado RA, Grabenstatter JD, Zuzow R, Morris A, Huang SY, Summons RE,

King N. 2013. *Algoriphagus machipongonensis* sp. nov., co-isolated with a

colonial choanoflagellate. Int J Syst Evol Microbiol 63:163–168.

29.   Matsuo Y, Suzuki M, Kasai H, Shizuri Y, Harayama S. 2003. Isolation and

phylogenetic characterization of bacteria capable of inducing differentiation

455   in the green alga *Monostroma oxyspermum*. Environ Microbiol 5:25–35.

30.   Grimes DJ, Johnson CN, Dillon KS, Flowers AR, Noriea NF, Berutti T. 2009.

What genomic sequence information has revealed about *Vibrio* ecology in the

ocean. Microb Ecol 58:447–460.

31.   Takemura AF, Chien DM, Polz MF. 2014. Associations and dynamics of

460   Vibrionaceae in the environment, from the genus to the population level.

Front Microbiol 5:1–26.

32.   Koropatnick TA, Engle JT, Apicella MA, Stabb E V., Goldman WE, McFall-Ngai

MJ. 2004. Microbial factor-mediated development in a host-bacterial

mutualism. Science 306:1186–1188.

465   33.   van der Heijden MG, Bruin S De, Luckerhoff L, van Logtestijn RS, Schlaeppi K.

2016. A widespread plant-fungal-bacterial symbiosis promotes plant

biodiversity, plant nutrition and seedling recruitment. ISME J 10:389–399.

34. Murray JL, Connell JL, Stacy A, Turner KH, Whiteley M. 2014. Mechanisms of synergy in polymicrobial infections. J Microbiol 52:188–199.

470   35. Trinchieri G, Sher A. 2007. Cooperation of Toll-like receptor signals in innate immune defence. Nat Rev Immunol 7:179–190.

36. Kroczek RA, Mages HW, Hutloff A. 2004. Emerging paradigms of T-cell co-stimulation. Curr Opin Immunol 16:321–327.
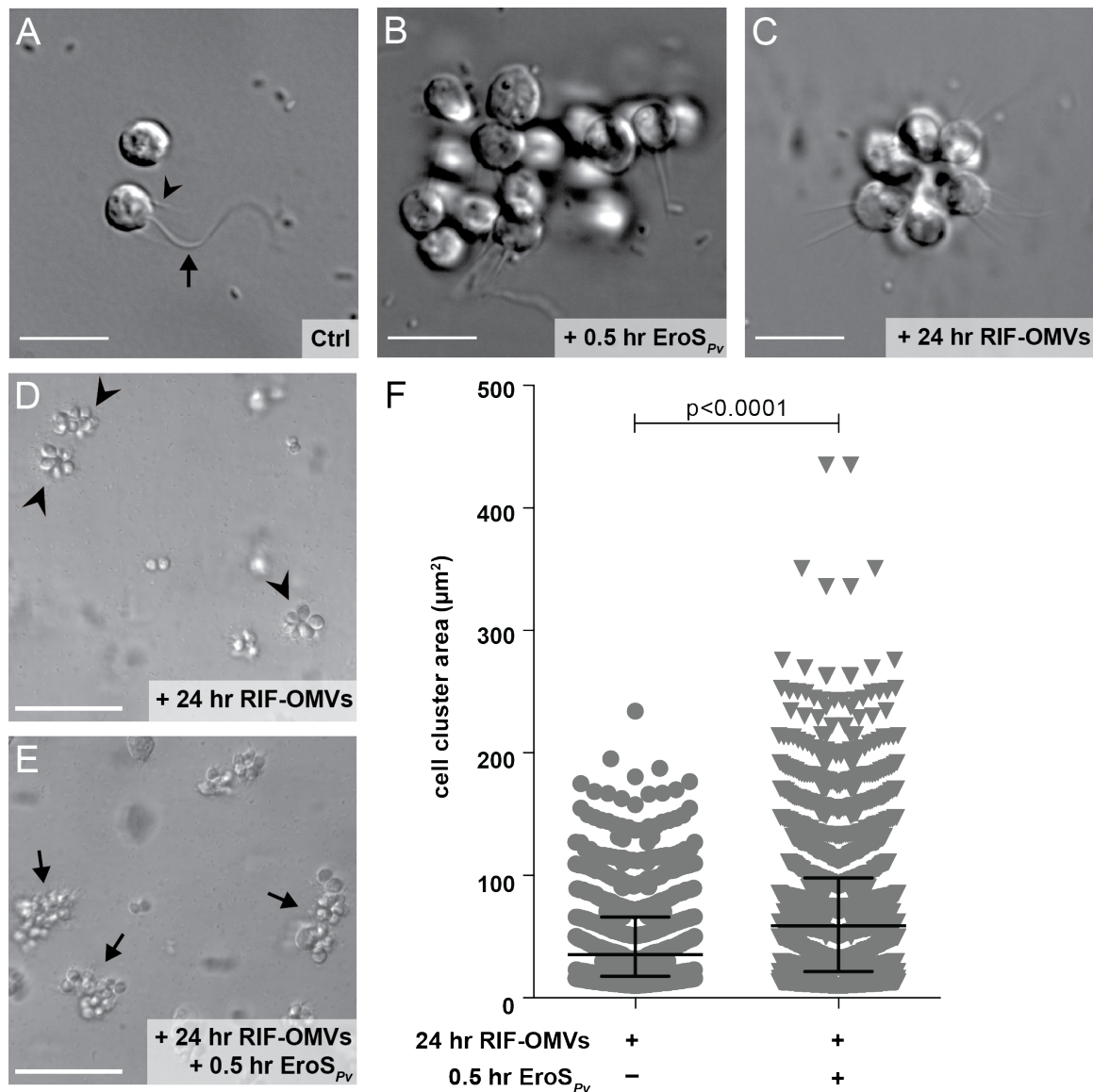
Figure 1: Rosettes swarm in response to the EroS$_{Pv}$ mating factor

(A-C) Bacterial cues regulate mating and multicellularity in *S. rosetta*. Scale bars = 10 μm. (A) *S. rosetta* grown in the presence of the prey bacterium *E. pacifica* ("Ctrl") proliferated as solitary cells. This culture served as the foundation for all experiments in this study. A typical *S. rosetta* cell has an apical collar (arrowhead) surrounding a single flagellum (arrow). (B) *S. rosetta* formed mating swarms within 0.5 hours of treatment with the bacterially-produced chondroitinase EroS$_{Pv}$. (C) *S.*

26

rosetta solitary cells developed into rosettes through serial rounds of cell division

within 24 hours of treatment with RIF-OMVs from the bacterium *A.*

machipongonensis. (D-E) Rosettes swarm in the presence, but not in the absence, of

485   EroS$_{Pv}$. Scale bars = 50 µm. (D) After 24 hours of treatment with RIF-OMVs, solitary

cells in an SrEpac culture developed into rosettes (arrowheads) but did not swarm.

(E) Swarms of rosettes (arrows) formed after 24 hours of treatment with RIF-OMVs

followed by 0.5 hours of treatment with EroS$_{Pv}$. (F) Shown are the surface areas of

cell clusters from SrEpac cultures treated with RIF-OMVs for 24 hours followed by

490   0.5 hours of incubation either with or without EroS$_{Pv}$. Following the approach of

(18), we generated a binary mask to measure cell cluster area (the area of each cell,

rosette, or swarm; Fig. S1). EroS$_{Pv}$ treatment resulted in clusters of cells, including

swarms of rosettes (median = 58.7 µm^2, interquartile range = 21.6-98.0 µm^2), whose

areas were significantly larger than those measured in the rosette-only control

495   (median = 35.5 µm^2, interquartile range = 17.8-65.9 µm^2) (Kolmogorov-Smirnov

test). 875 cell cluster areas were plotted for the cultures treated with RIF-OMVs and

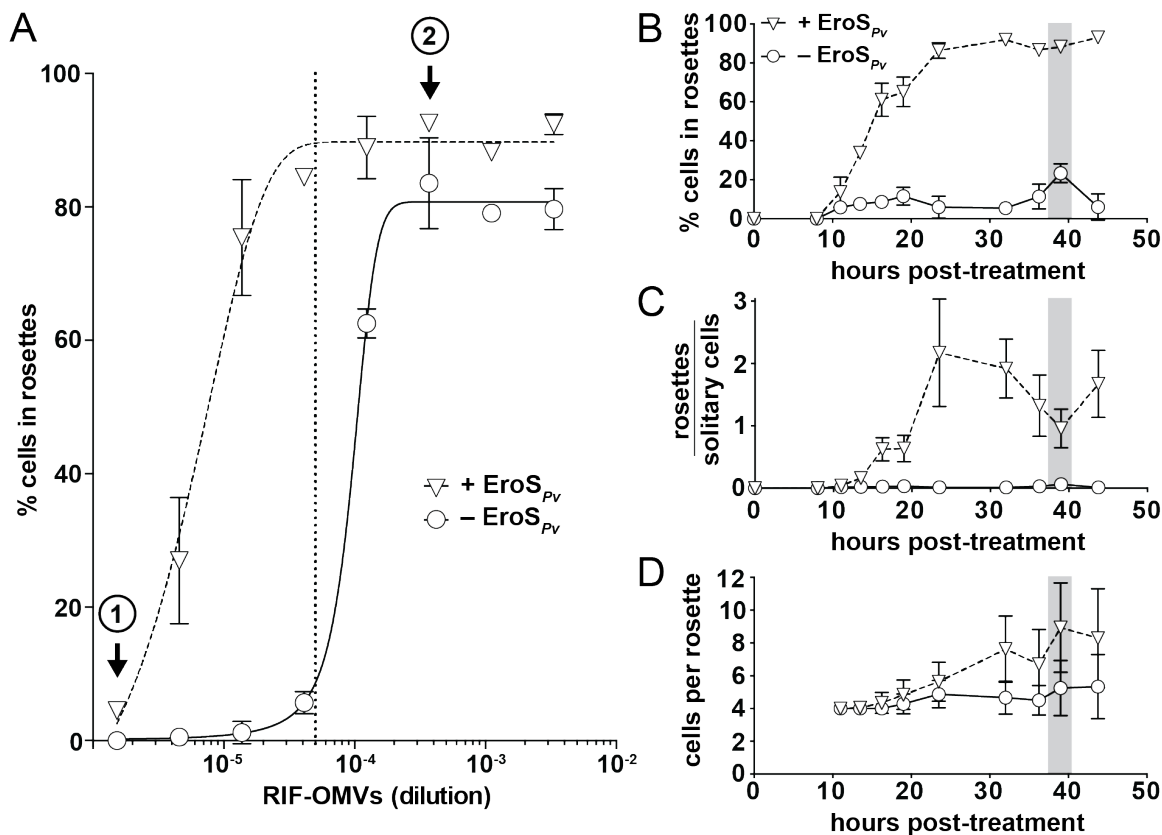1359 cell cluster areas were plotted for the cultures treated with RIF-OMVs + EroS$_{Pv}$.

Figure 2: The mating inducer EroS$_{Pv}$ enhances rosette development

(A) EroS$_{Pv}$ enhances rosette induction by RIF-OMVs. Treatment of SrEpac with

500   increasing concentrations of RIF-OMVs (circles) resulted in a concomitant increase

in the percentage of cells in rosettes. Co-treatment of SrEpac with RIF-OMVs and

0.05 U/mL EroS$_{Pv}$ (triangles) resulted in rosette development at concentrations of

RIF-OMVs that did not otherwise induce rosettes (e.g. at (**1**)). EroS$_{Pv}$ also increased

the maximum percentage of cells in rosettes at saturating concentrations of RIF-

505   OMVs (e.g. at (**2**)). The 1:20,000 dilution of RIF-OMVs used for the sensitized rosette

induction assays in panels B-D is indicated with a vertical dotted line. Mean plotted

± S.D. (B) Co-treatment of SrEpac with EroS$_{Pv}$ and RIF-OMVs leads to a dramatic

increase in percentage of cells in rosettes throughout the course of rosette

development relative to SrEpac treated only with RIF-OMVs. After 39 hours (shaded

510 bar) of co-treatment with RIF-OMVs and EroS$_{Pv}$ (triangles), 88.2±2.7% (mean ± S.D.)

of *S. rosetta* cells were in rosettes, compared with 23.4±4.9% (mean ± S.D.) of cells

treated with RIF-OMVs alone (circles). (C) EroS$_{Pv}$ increased the ratio of rosettes to

solitary cells in SrEpac cultures treated with RIF-OMVs. After 39 hours (shaded bar)

of co-treatment with RIF-OMVs and EroS$_{Pv}$ (triangles), the ratio of rosettes to

515 solitary cells was 0.96±0.31 (mean ± S.D.), compared with 0.06±0.02 (mean ± S.D.)

after treatment with RIF-OMVs alone (circles). (D) EroS$_{Pv}$ increased the number of

cells per rosette in RIF-OMV-treated SrEpac cultures. After 39 hours (shaded bar) of

co-treatment with RIF-OMVs and EroS$_{Pv}$ (triangles), there were 8.9±2.7 (mean ±

S.D.) *S. rosetta* cells per rosette colony, compared with 5.3±1.7 (mean ± S.D.) cells

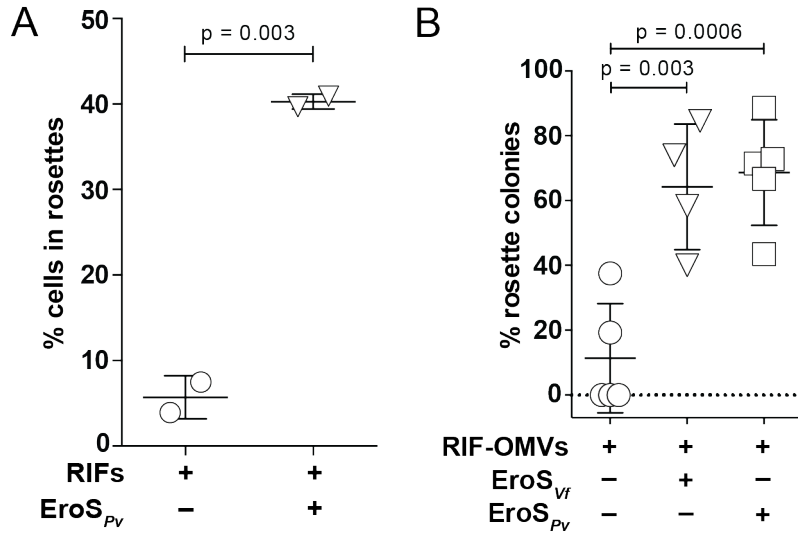520 per rosette colony after treatment with RIF-OMVs alone (circles).

Figure 3: Purified RIFs and EroS are sufficient for enhancement of rosette induction

(A) Co-treatment of SrEpac with 10 µg/mL HPLC-purified RIFs and 0.05 U/mL EroS$_{Pv}$ (triangles) resulted in an increase in the percentage of *S. rosetta* cells in rosettes compared to treatment with HPLC-purified RIFs alone (circles). Mean plotted ± S.D. (unpaired *t* test). (B) Co-treatment of SrEpac with a 1:20,000 dilution of RIF-OMVs and either 0.1% EroS from *V. fischeri* (EroS$_{Vf}$), or 0.05 U/mL EroS from *P. vulgaris* (EroS$_{Pv}$) resulted in an increase in the percentage of rosette colonies compared to treatment with RIF-OMVs alone. Mean plotted ± S.D. (unpaired *t* test).
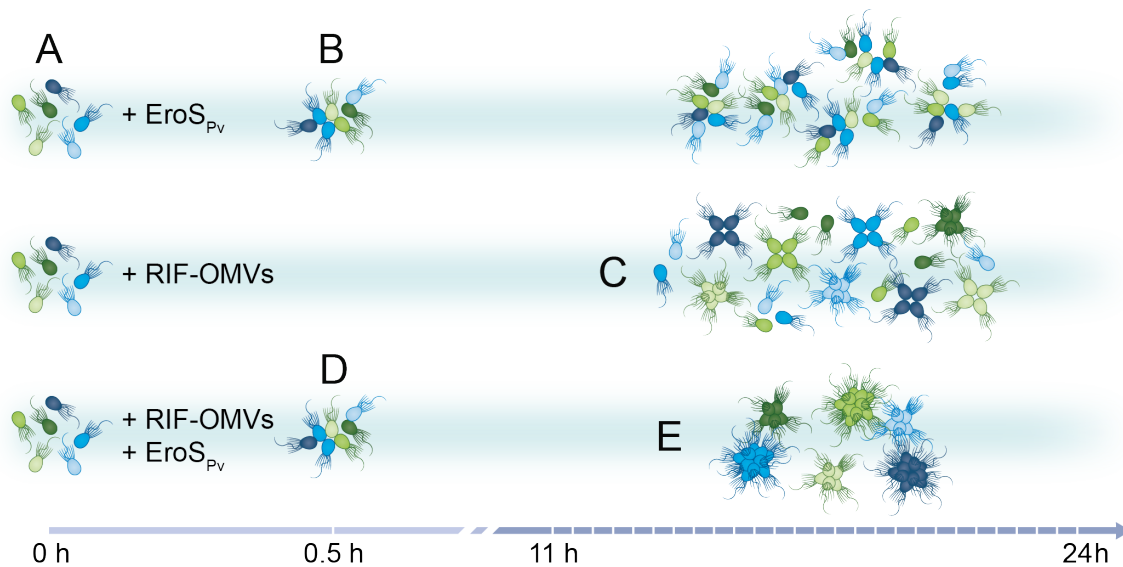
Figure 4: *S. rosetta* integration of bacterial cues

S. rosetta phenotypes induced over time by EroS$_{Pv}$, RIF-OMVs, and the synergistic effect of both cues. (A) Untreated SrEpac proliferates as solitary cells. (B) Treatment with EroS$_{Pv}$ induces swarming of unrelated cells within 0.5 hours. (C) Treatment with RIF-OMVs induces rosette development through cell division within 11-24 hours. (D) Co-treatment with RIF-OMVs and EroS$_{Pv}$ for 0.5 hours results in swarming, showing that RIF-OMVs do not interfere with or enhance the activity of EroS$_{Pv}$. (E) After 11-24 hours of co-treatment with RIF-OMVs and EroS$_{Pv}$, rosettes develop and swarm. Compared to treatment with RIF-OMVs alone, co-treatment with RIF-OMVs and EroS$_{Pv}$ induces the development of more rosettes and rosettes containing more cells.

31

Table 1: *S. rosetta* phenotypes induced by EroS$_{Pv}$ and RIF-OMVs

Bacterial cue	Hours after induction	*S. rosetta* phenotype	Effect on swarming	Effect on rosette development
EroS$_{Pv}$	0.5	swarming	induces	n/a
RIF-OMVs	0.5	solitary	none	n/a
EroS$_{Pv}$ + RIF-OMVs	0.5	swarming	induces	n/a
EroS$_{Pv}$	24	swarming	induces	none
RIF-OMVs	24	rosette	none	induces
EroS$_{Pv}$ + RIF-OMVs	24	rosette + swarming	induces	enhances

32

SUPPLEMENTAL MATERIAL

545

Synergistic cues from diverse bacteria enhance multicellular development in a choanoflagellate

Ella V. Ireland[a], Arielle Woznica[a,*] and Nicole King[a,b#]

550

[a]Department of Molecular and Cell Biology, University of California, Berkeley, California, USA

[b]Howard Hughes Medical Institute, University of California, Berkeley, California, USA

555   #Address correspondence to Nicole King, nking@berkeley.edu.

*Present address: Department of Microbiology, University of Texas Southwestern Medical Center, Dallas, Texas, USA
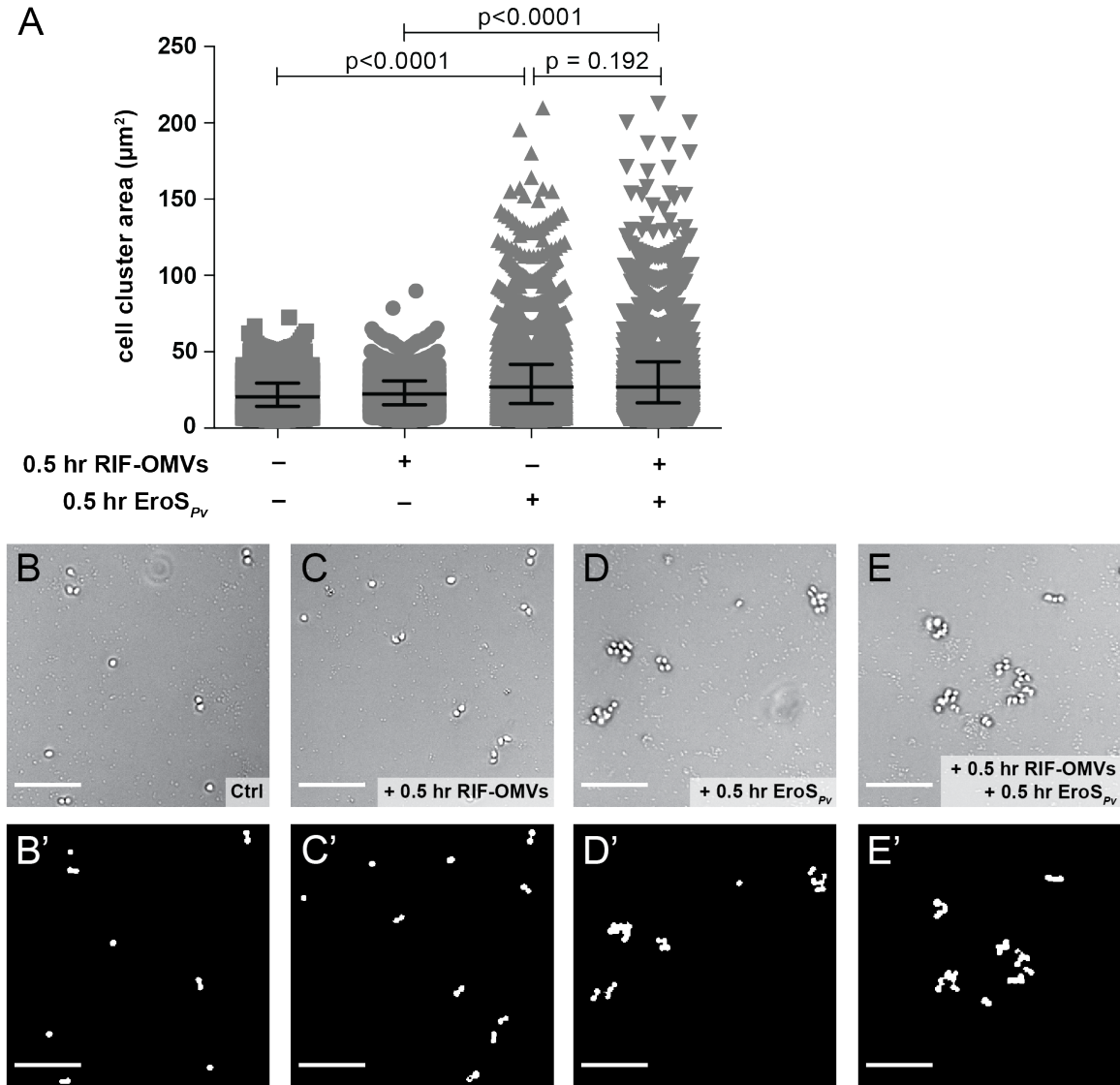
560

565

570

575

Figure S1: RIF-OMVs have no effect on EroS$_{Pv}$-induced swarming

(A) Solitary cells from SrEpac co-treated with RIF-OMVs and EroS$_{Pv}$ formed swarms, quantifiable by an increase in cell cluster area (median = 27.0 μm^2, interquartile range = 16.5-43.5 μm^2) compared to cells treated with RIF-OMVs alone (median = 22.4 μm^2, interquartile range = 15.2-30.8 μm^2). There was no significant difference in swarm size between cells co-treated with RIF-OMVs and EroS$_{Pv}$ and cells treated with EroS$_{Pv}$ alone (median = 27.0 μm^2, interquartile range = 16.0-41.8 μm^2)

580

34

(Kolmogorov-Smirnov test). A minimum of 2730 cell cluster areas were plotted for

585   each condition. (B-E') Sample images used for quantification in (A). Following the

approach of (18), raw images in (B-E) were converted to binary images (B'-E') to

measure cell cluster size (Materials and Methods). (B) *S. rosetta* cells from untreated

SrEpac remained solitary. (C) *S. rosetta* cells from SrEpac treated with RIF-OMVs for

0.5 hours remained solitary. (D) *S. rosetta* cells from SrEpac treated with EroS$_{Pv}$ for

590   0.5 hours formed visible swarms. (E) *S. rosetta* cells from SrEpac co-treated with

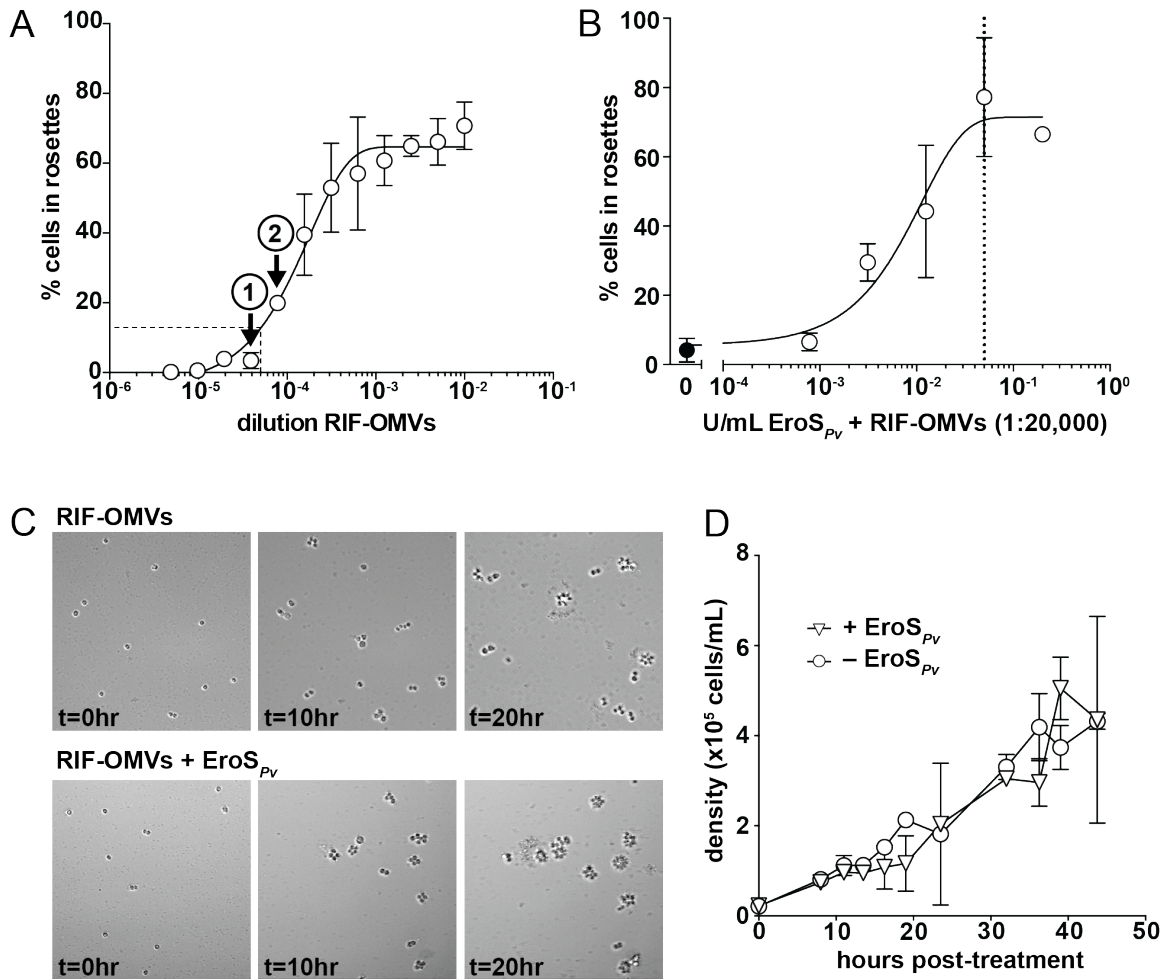RIF-OMVs and EroS$_{Pv}$ for 0.5 hours formed visible swarms.

Figure S2: EroS$_{Pv}$ enhances rosette development, but not cell proliferation, in a sensitized rosette induction assay

595 (A) Serial dilution of RIF-OMVs can be used to induce a low percentage of cells in rosettes. SrEpac treated with a 1:25,600 dilution of RIF-OMVs resulted in 3.4±2.3 (mean ± S.D.) *S. rosetta* cells in rosettes (arrow marked (**1**)), while a 1:12,800 dilution of RIF-OMVs resulted in 19.9±1.7 (mean ± S.D.) *S. rosetta* cells in rosettes (arrow marked (**2**)). An intermediate dilution of 1:20,000 was used for the sensitized rosette induction assay (dashed lines). (B) Rosette-enhancing activity

600

correlated with EroS$_{Pv}$ concentration. SrEpac treated with a 1:20,000 dilution of RIF-OMVs (black circle) contained more *S. rosetta* cells in rosettes upon the addition of increasing concentrations of EroS$_{Pv}$ (white circles). Dotted line indicates concentration of EroS$_{Pv}$ (0.05 U/mL) used for subsequent assays. Mean plotted ± S.D.

605 (C) Time-lapse imaging showed an increase in both the number of rosettes and the number of cells per rosette after co-treatment with a 1:20,000 dilution of RIF-OMVs and 0.05 U/mL EroS$_{Pv}$ (bottom) compared to RIF-OMVs alone (top). (D) *S. rosetta* cells treated with RIF-OMVs (circles) or co-treated with RIF-OMVs and EroS$_{Pv}$ (triangles) grew at the same rate. Mean density plotted ± S.D.